

CEBAF



0205 9100 017 084 4

# CEBAF

The Continuous Electron Beam Accelerator Facility

Theory Group Preprint Series

CEBAF-TH-94-27

Additional copies are available from the authors.

The Southeastern Universities Research Association (SURA) operates the Continuous Electron Beam Accelerator Facility for the United States Department of Energy under contract DE-AC05-84ER40150

## A Strange Mesonic Transition Form Factor \*

J. L. Goity

*Department of Physics, Hampton University, Hampton, VA 23668, and  
Theory Group, MS 12112, Continuous Electron Beam Accelerator Facility,  
Newport News, VA 23606, U.S.A.*

M. J. Musolf<sup>1</sup>

*Department of Physics, Old Dominion University Norfolk, VA 23529, and  
Theory Group, MS 12112 Continuous Electron Beam Accelerator Facility,  
Newport News, VA 23606, U.S.A.*

The strange-quark vector current  $\rho$ -to- $\pi$  meson transition form factor is computed at one-loop order using strange meson intermediate states. A comparison is made with a  $\phi$ -meson dominance model estimate. We find that one-loop contributions are comparable in magnitude to those predicted by  $\phi$ -meson dominance. It is possible that the one-loop contribution can make the matrix element as large as those of the electromagnetic current mediating vector meson radiative decays. However, due to the quadratic dependence of the one-loop results on the hadronic form factor cut-off mass, a large uncertainty in the estimate of the loops is unavoidable. These results indicate that non-nucleonic strange quarks could contribute appreciably in moderate- $|Q^2|$  parity-violating electron-nucleus scattering measurements aimed at probing the strange-quark content of the nucleon.

### DISCLAIMER

This report was prepared as an account of work sponsored by the United States government. Neither the United States nor the United States Department of Energy, nor any of their employees, makes any warranty, express or implied, or assumes any legal liability or responsibility for the accuracy, completeness, or usefulness of any information, apparatus, product, or process disclosed, or represents that its use would not infringe privately owned rights. Reference herein to any specific commercial product, process, or service by trade name, mark, manufacturer, or otherwise, does not necessarily constitute or imply its endorsement, recommendation, or favoring by the United States government or any agency thereof. The views and opinions of authors expressed herein do not necessarily state or reflect those of the United States government or any agency thereof.

\*This work is supported in part by funds provided by the U. S. Department of Energy (D.O.E.) under contracts #DE-AC05-84ER40150 and #DE-FG05-94ER0832.

<sup>1</sup>National Science Foundation Young Investigator

# A Strange Mesonic Transition Form Factor \*

J. L. Goily

*Department of Physics, Hampton University, Hampton, VA 23668, and  
Theory Group, MS 12H2, Continuous Electron Beam Accelerator Facility,  
Newport News, VA 23606, U.S.A.*

M. J. Musolf<sup>†</sup>

*Department of Physics, Old Dominion University Norfolk, VA 23529, and  
Theory Group, MS 12H2 Continuous Electron Beam Accelerator Facility,  
Newport News, VA 23606, U.S.A.*

The strange-quark vector current  $\rho$ -to- $\pi$  meson transition form factor is computed at one-loop order using strange meson intermediate states. A comparison is made with a  $\phi$ -meson dominance model estimate. We find that one-loop contributions are comparable in magnitude to those predicted by  $\phi$ -meson dominance. It is possible that the one-loop contribution can make the matrix element as large as those of the electromagnetic current mediating vector meson radiative decays. However, due to the quadratic dependence of the one-loop results on the hadronic form factor cut-off mass, a large uncertainty in the estimate of the loops is unavoidable. These results indicate that non-nucleonic strange quarks could contribute appreciably in moderate- $|Q^2|$  parity-violating electron-nucleus scattering measurements aimed at probing the strange-quark content of the nucleon.

## I. INTRODUCTION

There has been considerable interest recently in the use of semi-leptonic weak neutral current scattering to study the strange-quark "content" of the nucleon [1-12]. In particular, several parity-violating (PV) electron scattering experiments are planned and/or underway at MIT-Bates, CEBAF, and MAINZ whose objective is to measure the nucleon's strange-quark vector current form factors [13-17]. In a similar vein, a low- $|Q^2|$  determination of the nucleon's axial vector strangeness form factor will be made using neutrino scattering at LAMPF [18], following on the higher- $|Q^2|$  measurement made at Brookhaven [19]. These experiments are of interest in part because they provide a new window on the role played by non-valence degrees of freedom (specifically, virtual  $s\bar{s}$  pairs) in the nucleon's response to a low- or medium-energy external probe. In contrast to the theoretical analysis of scattering in the deep inelastic regime, for which perturbative methods are applicable, the interpretation of low-to-medium energy scattering can be carried out at present only within the context of effective hadronic models. In the case of the nucleon's strangeness form factors, several model calculations have been performed yielding a rather broad spectrum of results [20-26]. It is desirable, then, that experimental determinations of these form factors be carried out at a level of precision allowing one to distinguish among various models and the physical pictures on which they are based.

As discussed elsewhere in the literature, semi-leptonic measurements performed with proton targets alone would not be sufficient for this purpose [1, 2, 6]. A program of measurements which includes  $A > 1$  targets appears to be warranted [1, 2]. The interpretation of neutrino-nucleus and PV electron-nucleus

---

\*This work is supported in part by funds provided by the U. S. Department of Energy (D.O.E.) under contracts #DE-AC05-84ER40150 and #DE-FG05-94ER0832.

<sup>†</sup>National Science Foundation Young Investigator

scattering observables naturally introduces a new level of complication associated with many-body nuclear dynamics not encountered in the case of proton targets. These many-body effects are interesting in two respects. On the one hand, if one wishes to extract the single nucleon strangeness form factors from nuclear form factors, one requires knowledge of the many-body contributions to the nuclear strangeness form factors. On the other, the role played by non-nucleonic strangeness (i.e., non-nucleonic, non-valence quark degrees of freedom) in the nuclear response is interesting in its own right.

Recently, one class of many-body contributions to the nuclear strangeness form factors – meson exchange currents (MEC's) – were analyzed for the case of  $^4\text{He}$  [27, 28]. A helium target will be used in a future CEBAF PV electron scattering experiment designed to study the nucleon's strangeness electric form factor at moderate- $|Q^2|$  [14]. In Ref. [28], it was shown that MEC's give a non-negligible contribution to the  $^4\text{He}$  strangeness form factor at the kinematics of the approved experiment. Of particular note is the  $\rho$ -to- $\pi$ -meson strange-quark "transition current". Using a simple  $\phi$ -meson vector dominance model and the known  $\phi \rightarrow \rho\pi$  branching ratio, this MEC was estimated to give a 15% contribution to the PV asymmetry. Given the magnitude of this result and its potential importance in the interpretation of the  $^4\text{He}$  experiment, one would like a more detailed analysis of this strangeness transition current. The goal of the present paper is to improve upon the vector dominance estimate by including loop effects. In so doing, our objective is not so much to provide an airtight theoretical prediction as to arrive at an order of magnitude for, and quantify the theoretical uncertainty associated with, loop effects. Section II gives a brief discussion of the nuclear physics context for our calculation as well as a review of the  $\phi$ -dominance estimate of the  $\rho$ - $\pi$  strangeness form factor. In Section III we present the formal framework in which we carry out our analysis. The loop calculation is presented in Section IV. Section V gives our results and a discussion of their significance, and in Section VI we summarize our work. Technical details may be found in the Appendix.

## II. NUCLEAR STRANGENESS FORM FACTORS

The  $^4\text{He}$  PV asymmetry,  $A_{LN}$ , can be written as [1, 2, 6]

$$A_{LN} = \frac{G_\mu |Q^2|}{4\sqrt{2}\pi\alpha} \left[ 4\sin^2\theta_w + \frac{F_C^{(s)}(q)}{F_C^{T=0}(q)} \right], \quad (1)$$

where  $G_\mu$  is the Fermi constant measured in  $\mu$ -decay,  $Q^2 = \omega^2 - |\vec{q}|^2$  is the four-momentum transfer squared, and where electroweak radiative corrections have been ignored for simplicity. The quantity  $F_C^{T=0}(q)$  is the  $^4\text{He}$  electromagnetic elastic charge form factor ( $T = 0$  for isoscalar targets). The  $^4\text{He}$  elastic strangeness form factor,  $F_C^{(s)}(q)$ , is given by

$$F_C^{(s)}(q) = \int d^3x e^{i\vec{q}\cdot\vec{x}} \langle \text{g.s.} | s^\dagger(\vec{x}) s(\vec{x}) | \text{g.s.} \rangle, \quad (2)$$

where  $|\text{g.s.}\rangle$  is the nuclear ground state and  $s(\vec{x})$  is the strange-quark field operator. Note that since  $s^\dagger s$  is just the charge component of the strangeness vector current,  $\bar{s}\gamma_\mu s$ , and since  $^4\text{He}$  has no net strangeness, the form factor  $F_C^{(s)}$  must vanish at zero momentum transfer. For non-zero momentum transfer,  $F_C^{(s)}(q)$  receives a number of contributions, some of which are illustrated in Fig. 1.

In conventional (non-relativistic) nuclear models, the processes of Figs. 1a and 1b are sensitive to the nucleon's strangeness vector current form factors. Those of type 1a give the so-called impulse approximation, or one-body, contribution. Processes of type 1b which involve an exchange of a meson  $M$  must be included in any nuclear calculation which respects vector current conservation and in which the two-nucleon potential arises from the exchange of meson  $M$ . In the present paper, we are concerned with contributions of type 1c, which involve matrix elements of the strangeness vector current between meson states  $M$  and  $M'$ . It is straightforward to show using G-parity invariance that  $\langle M' | \bar{s}\gamma_\mu s | M \rangle$  vanishes when  $M = M'$ . Hence, only transition matrix elements contribute. The corresponding MEC's are referred to as "transition currents". For moderate values of momentum-transfer, one expects the lightest mesons to give the largest effect, since they have the longest range and experience the least suppression from the  $N - N$  short range repulsion. For this reason, we restrict our attention to the transition current involving the lightest possible allowed pair of states:  $M = \pi$  and  $M' = \rho$ .

For on-shell mesons, the  $\rho$ -to- $\pi$  transition matrix element has the structure

$$\langle \rho^a(k_1, \epsilon) | \bar{s}\gamma_\mu s | \pi^b(k_2) \rangle = \frac{g_{\rho\pi}^{(s)}(Q^2)}{M_\rho} \epsilon_{\mu\nu\alpha\beta} k_1^\nu k_2^\alpha \epsilon^{\beta*} \delta^{ab}, \quad (3)$$

where  $\varepsilon^\beta$  is the  $\rho$ -meson polarization vector,  $k_1$  and  $k_2$  are the meson momenta, and  $a$  and  $b$  are isospin indices. In the case of nuclear processes, where the typical momenta of hadrons inside the nucleus have magnitudes less than the Fermi momentum ( $\sim 200$  MeV), the virtual  $\rho$ -meson will be rather far off its mass shell. Consequently, the dimensionless form factor  $g_{\rho\pi}^{(s)}$  ought also to depend on  $k_1^2$  and  $k_2^2$  as well as  $Q^2$ . It is conventional in nuclear calculations, however, to neglect the off-shell dependence of transition form factors, so for purposes of making contact with this framework, we will quote results for the on-shell case.

In previous work [27, 28], an estimate of  $g_{\rho\pi}^{(s)}(Q^2)$  was made based on the assumption of  $\phi$ -meson dominance, as illustrated in Fig. 2. Under this assumption, one has

$$\langle \rho^a(k_1, \varepsilon) | \bar{s} \gamma_\mu s | \pi^b(k_2) \rangle = \langle 0 | \bar{s} \gamma_\mu s | \phi(Q, \varepsilon_\phi) \rangle \frac{1}{Q^2 - M_\phi^2} \langle \phi(Q, \varepsilon_\phi) | \rho(-k_1, \varepsilon) \pi(k_2) \rangle, \quad (4)$$

where  $\varepsilon_\phi$  is the virtual  $\phi$ -meson polarization vector and where a sum over all independent polarizations is implied. Noting that the  $\phi$  is nearly a pure  $s\bar{s}$  state, so that  $\langle 0 | \bar{u} \gamma_\mu u | \phi \rangle \approx 0 \approx \langle 0 | \bar{d} \gamma_\mu d | \phi \rangle$ , one has (see the Appendix for details)

$$\langle 0 | \bar{s} \gamma_\mu s | \phi(Q, \varepsilon) \rangle \approx -3 \langle 0 | J_\mu^{SM} | \phi(Q, \varepsilon) \rangle = -3 \frac{M_\phi^2}{f_\phi} \varepsilon_\mu, \quad (5)$$

where one obtains  $f_\phi \approx 13$  from an analysis of  $\Gamma(\phi \rightarrow e^+ e^-)$  [29]. From the experimental value for the  $\phi \rightarrow \rho\pi$  branching ratio [29], one may obtain a value for the magnitude of the decay amplitude,  $\langle \rho\pi | \phi \rangle$ . From these inputs one obtains for the transition form factor (see the Appendix)

$$g_{\rho\pi}^{(s)}(Q^2) \Big|_{\phi\text{-dom}} = \frac{g_{\rho\pi s}}{Q^2 - M_\phi^2}, \quad (6)$$

with  $|g_{\rho\pi s}| \approx 0.20 \text{ GeV}^2$  [30].

In what follows, we consider additional contributions to  $g_{\rho\pi}^{(s)}(Q^2)$  arising from loops, as in Fig. 3.

The rationale for considering these contributions is similar to that for including loops in studies of other form factors. From a dispersion integral standpoint,  $g_{\rho\pi}^{(s)}(Q^2)$  receives contributions not only from poles (identified with vector

mesons), but also from the multi-meson, intermediate-state continuum. For values of  $Q^2$  sufficiently far from the poles (e.g.,  $M_\phi^2$ ), the continuum contributions need not be negligible. In the present instance, the lightest allowed intermediate states contain one pseudoscalar and one vector meson (parity requires the vanishing of the strong interaction  $\pi \rightarrow$  two  $K$  amplitude). Hence, we will consider contributions involving one  $K$  and one  $K^*$  in the intermediate state.

### III. EFFECTIVE LAGRANGIANS

In this section we derive the effective interactions relevant to the calculation of one-loop contributions to the matrix element  $\langle \rho^a(k_1, \varepsilon) | \bar{s} \gamma_\mu s | \pi^b(k_2) \rangle$  and determine the effective coupling constants associated with them. In the derivation we use an effective chiral Lagrangian, which takes into account the global symmetries of QCD. This Lagrangian involves the octet of light pseudoscalar mesons (the quasi-Goldstone bosons of spontaneously broken chiral  $SU_L(3) \times SU_R(3)$ ), the nonet of vector mesons, and external gauge sources needed to obtain the relevant currents (electromagnetic and strangeness) which play a role in our analysis.

The framework is that of the non-linear  $\sigma$ -model. The quasi-Goldstone fields are coordinates of the coset space  $SU_L(3) \times SU_R(3) / SU_V(3) \sim SU(3)$ , and appear in the following form

$$U(x) = \exp\left(-i \frac{\Pi}{F_0}\right), \quad \Pi = \sum_{a=1}^8 \pi^a \lambda^a, \quad (7)$$

where  $\lambda^a$  are the Gell-Mann matrices normalized according to  $\text{Tr}(\lambda^a \lambda^b) = 2 \delta^{ab}$ ,  $\pi^a$  are the members of the octet of pseudoscalar quasi-Goldstone fields, and  $F_0 \sim 93$  MeV is the pion decay constant in the chiral limit. The transformation properties of the quasi-Goldstones are determined by the way  $U(x)$  responds to a chiral transformation:  $U(x) \rightarrow R U(x) L^\dagger$ , where  $L$  ( $R$ ) belongs to  $SU_L(3)$  ( $SU_R(3)$ ).

The chiral transformation law for the octet of vector mesons is given by

$$V_\mu \rightarrow h V_\mu h^\dagger \quad (8)$$

where  $V_\mu = V_\mu^a \lambda^a$ ,  $u(x) \equiv \sqrt{U(x)}$ , and  $h = h(L, R, u(x))$  is determined by the equations

$$L u(x) = u'(x) h \quad R u^1(x) = u'^1(x) h, \quad (9)$$

where  $u'$  results from the action of the chiral transformation on  $u$ .

In order to build a chirally invariant Lagrangian for the octet of vector mesons we further need to introduce a covariant derivative

$$\nabla_\mu = \partial_\mu - i \Gamma_\mu \quad \Gamma_\mu = \frac{i}{2} (u^\dagger \partial_\mu u + u \partial_\mu u^\dagger), \quad (10)$$

which operates as follows on  $V_\mu$ :  $\nabla_\mu V_\nu = \partial_\mu V_\nu - i [\Gamma_\mu, V_\nu]$ . Similarly, we require the axial vector connection

$$\omega_\mu = \frac{i}{2} (u^\dagger \partial_\mu u - u \partial_\mu u^\dagger). \quad (11)$$

Both  $\nabla_\mu$  and  $\omega_\mu$  have the same chiral transformation law as  $V_\mu$ .

In addition, we will consider two external source gauge fields, the electromagnetic potential  $A_\mu$  and the potential  $S_\mu$  which couples to the strangeness vector current. In this way one can obtain the most general form of the respective currents in the effective theory. At the appropriate stage we will show how they enter in the effective Lagrangian.

The piece of the effective Lagrangian containing the kinetic and mass terms of the vector meson octet is given by

$$\mathcal{L}_V = -\frac{1}{8} \text{Tr}(V_{\mu\nu} V^{\mu\nu}) + \frac{M_V^2}{4} \text{Tr}(V_\mu V^\mu) \quad , \quad (12)$$

where  $V_{\mu\nu} = \nabla_\mu V_\nu - \nabla_\nu V_\mu$ . The Lagrangian  $\mathcal{L}_V$  only contains terms with two vector mesons ( $V$ ) and even numbers of quasi-Goldstone bosons ( $P$ ). There is no  $SU(3)$  breaking at this level in the interactions. For simplicity, we will only include the dominant  $SU(3)$  breaking effects which are generated by the mass splittings in the octets of pseudoscalar and vector mesons.

The vertex of type  $VVP$  needed in our analysis is specifically  $\rho K^* K$ . In order to determine the corresponding coupling constant we need to consider in addition the  $VV^0 P$  vertices, where  $V^0$  is the singlet component of the nonet of vector mesons. The corresponding effective Lagrangians at leading order in chiral power counting are of  $\mathcal{O}(p)$ , where  $p$  denotes the generic small momentum carried by the quasi-Goldstone bosons, and read

$$\begin{aligned} \mathcal{L}_{VVP} &= R_8 \epsilon_{\mu\nu\rho\sigma} \text{Tr}(\{\nabla^\mu V^\nu, V^\rho\} \omega^\sigma) \\ \mathcal{L}_{VV^0P} &= R_0 \epsilon_{\mu\nu\rho\sigma} \text{Tr}(\nabla^\mu V^\nu \omega^\rho) V^{0\sigma} \end{aligned} \quad (13)$$

Here, we have used the identity  $\epsilon_{\mu\nu\rho\sigma} \nabla^\rho \omega^\sigma = 0$  to simplify the expressions. For the vertices of interest we need only keep the first term in the expansion of  $\omega^\mu$ :  $\omega^\mu = \frac{1}{2F_0} \partial^\mu \Pi + \mathcal{O}(\Pi^3)$ . The only observable strong interaction process of this type is  $\phi \rightarrow \rho\pi$ . In order to be able to determine  $R_8$ , we must simultaneously pin down  $R_0$ , and this requires further information, which we obtain by considering the radiative decays  $V \rightarrow P\gamma$  supplemented with the hypothesis of vector meson dominance. From this analysis, presented in the Appendix, we obtain  $R_8 = 0.27 \pm 0.08$ .

The vertices of type  $VPP$  we need are of the type  $K^* K\pi$ . They are determined in terms of a single effective coupling, and the corresponding effective Lagrangian is

$$\mathcal{L}_{VPP} = \xi_8 \text{Tr}(\nabla_\mu V_\nu [\omega^\mu, \omega^\nu]) \quad , \quad (14)$$

where  $\xi_8$  can be determined from either of the following two decay widths:

$$\begin{aligned} \Gamma(\rho^0 \rightarrow \pi^+ \pi^-) &= \frac{\xi_8^2}{192\pi F_0^4} M_\rho^2 (M_\rho^2 - 4M_\pi^2)^{3/2} \\ \Gamma(K^{*+} \rightarrow K^+ \pi^0) &= \frac{\xi_8^2}{96\pi F_0^4} E_K E_\pi k_f (M_{K^*}^2 - (1 + \frac{E_\pi}{E_K}) M_K^2 - (1 + \frac{E_K}{E_\pi}) M_\pi^2) \\ k_f &= \frac{1}{2M_{K^*}} \sqrt{\lambda[M_{K^*}^2, M_K^2, M_\pi^2]} \quad , \end{aligned} \quad (15)$$

where  $\lambda[x, y, z] = x^2 + y^2 + z^2 - 2xy - 2xz - 2yz$ . The first width gives  $\xi_8 = 0.175$  and the second gives  $\xi_8 = 0.140$ . Notice that we have used the same decay constant for  $\pi$  and  $K$  mesons. Under the assumption of  $SU(3)$  symmetry in the interactions, the use of either value of  $\xi_8$  is justified.

Now we turn to those terms in the effective Lagrangian which determine the electromagnetic and strangeness currents. The electric charge operator contains only octet pieces and is explicitly given by  $\hat{Q} = \frac{e}{2}(\lambda^3 + \frac{1}{\sqrt{3}} \lambda^8) = \frac{e}{2} \text{diag}(2, -1, -1)$ , while the strangeness charge operator contains a singlet and an octet piece and reads  $\hat{S} = \frac{1}{3}(1 - \sqrt{3} \lambda^8) = \text{diag}(0, 0, 1)$ . In the following,  $\hat{q}$  denotes either of these charge operators, and  $v_\mu$  represents either of the two source fields  $A_\mu$  and  $S_\mu$ .

Let us first consider the  $V \rightarrow v_\mu$  amplitudes relevant for the VMD analysis. The effective Lagrangian contains an octet and a singlet piece

$$\mathcal{L}_{Vv} = C_8 v^\mu \text{Tr}(\hat{q} V_\mu) + C_0 v^\mu \text{Tr}(\hat{q}) V_\mu^0 \quad (16)$$

The leptonic widths of  $\rho^0$ ,  $\omega$  and  $\phi$  determine  $C_8$  according to:

$$\Gamma(V \rightarrow e^+ e^-) = \frac{4\pi}{3} \alpha^2 \frac{M_V}{f_V^2} \quad (17)$$

where

$$\begin{aligned} f_\rho &= \frac{\sqrt{2} M_\rho^2}{C_8} \\ f_\omega &= \frac{\sqrt{6} M_\omega^2}{\cos \theta C_8} \\ f_\phi &= \frac{\sqrt{6} M_\phi^2}{\sin \theta C_8} \end{aligned} \quad (18)$$

In practice, the  $\omega$ - $\phi$  mixing angle is taken to be that of ideal mixing,  $\tan \theta = \sqrt{2}$ , which leads to  $C_8 \simeq 0.18 \text{ GeV}^2$ . In order to determine the transition mediated by the strangeness current, we also need to know the singlet coupling  $C_0$ . As there is no direct experimental determination of this coupling, one must rely on some hypothesis. By assuming exact OZI suppression in the  $\omega$ -to-vacuum current matrix elements (i.e.,  $\langle 0 | \bar{s} \gamma_\mu s | \omega \rangle = 0$ ), we obtain  $C_0 = -C_8/\sqrt{3} = -0.092 \text{ GeV}^2$ .

The transitions within the octet of pseudoscalar and of vector mesons mediated by the currents are obtained by minimal substitution into the chiral covariant derivative  $\nabla_\mu$  in Eq. (12), plus a gauge invariant term involving the field strength tensor of the gauge field in the case of the vector mesons. Both electromagnetic and strangeness current transitions are determined by the following effective Lagrangians:

$$\begin{aligned} \mathcal{L}_{PPv} &= -\frac{i}{2} \text{Tr}(\partial_\mu \Pi [\hat{q}, \Pi] + \dots) v^\mu \\ \mathcal{L}_{VVv} &= \frac{i}{4} \text{Tr}(V_{\mu\nu} [\hat{q}, V^\nu]) v^\mu + i \frac{z}{2} \text{Tr}([V_\mu, V_\nu] \hat{q}) v^{\mu\nu} \end{aligned} \quad (19)$$

Only one new unknown effective coupling ( $z$ ) enters, which is related to the magnetic moments of the vector mesons. As we mention in the Section V, the

lack of experimental access to  $z$  does not affect our results, as it appears only in a loop diagram (diagram 3c) which turns out to be numerically substantially smaller than the other diagrams.

Vertices of type  $VPPv$  are obtained from Eq. (14) by minimal substitution in  $\nabla_\mu$  and  $\omega_\mu$ , and by a term proportional to the field strength tensor of the gauge field. The effective Lagrangian reads (for the sake of simplicity we keep only terms relevant to our calculation):

$$\begin{aligned} \mathcal{L}_{VPPv} &= -i \frac{\zeta_8}{4 F_0^2} \text{Tr}(\partial^\mu V^\nu ([\partial_\mu \Pi, [\hat{q}, \Pi]] v_\nu - \mu \leftrightarrow \nu) \\ &\quad + v^\mu [\hat{q}, V^\nu] [\partial_\mu \Pi, \partial_\nu \Pi]) \\ &\quad + i \frac{\zeta_8}{4 F_0^2} \text{Tr}(\partial^\mu V^\nu [[\hat{q}, \Pi], \Pi]) v_{\mu\nu} + \dots \end{aligned} \quad (20)$$

The new coupling constant  $\zeta_8$  is fixed by considering the radiative decay  $\rho^0 \rightarrow \pi^+ \pi^- \gamma$ . Using the expression for the partial width

$$\begin{aligned} \Gamma(\rho^0 \rightarrow \pi^+ \pi^- \gamma) &= \frac{\alpha M_\rho}{24 \pi^2 F_0^4} \int_{M_\pi}^{M_\rho} dE_1 \int_{M_\pi}^{M_\rho - E_1} dE_2 \\ &\quad \times \Theta [4(E_1^2 - M_\pi^2)(E_2^2 - M_\pi^2) \\ &\quad - (M_\rho^2 + 2M_\pi^2 - 2(E_1 + E_2)M_\rho + 2E_1 E_2)^2] \\ &\quad \times (2\zeta_8 M_\rho - (2\zeta_8 - \xi_8)(E_1 + E_2))^2 \end{aligned} \quad (21)$$

and using the previously determined value  $\xi_8 = 0.175$ , we obtain two solutions:  $\zeta_8 = 0.156$  and  $\zeta_8 = -0.082$ . Unfortunately, there are no further measured observables to discriminate between these two solutions. In our results we will include both possibilities.

The final vertices we need are those of the type  $VVPv$ . As in the previous case, we only need those involving members of the meson octets. They are entirely determined by minimal substitution into eq. (13), and the relevant pieces read:

$$\begin{aligned} \mathcal{L}_{VVPv} &= -i \frac{\kappa_8}{2 F_0} \epsilon_{\mu\nu\rho\sigma} \text{Tr}(v^\mu [[\hat{q}, V^\nu], V^\rho] \partial^\sigma \Pi \\ &\quad + v^\sigma \{\partial^\mu V^\nu, V^\rho\} [\hat{q}, \Pi]) \end{aligned} \quad (22)$$

We notice here that the effective Lagrangians (19), (20) and (22) only couple the octet components of the vector sources to the mesons. The SU(3) singlet piece of the vector current is the Baryon number current which cannot couple to mesons.

From the effective Lagrangians given in this section, it is straightforward to derive the Feynman rules and calculate the one-loop diagrams in the following section.

#### IV. ONE LOOP CALCULATION

In this section we discuss some salient features of the calculation of the one-loop contributions to  $\langle \rho^0(k_1, \varepsilon) | \bar{s} \gamma_\mu s | \pi^0(k_2) \rangle$ , which on grounds of isospin symmetry are the same as the contributions to  $\langle \rho^+(k_1, \varepsilon) | \bar{s} \gamma_\mu s | \pi^+(k_2) \rangle$ .

There are only four diagrams, depicted in Fig. 3, which contribute at one-loop order. As expected, all diagrams are ultraviolet divergent. Diagrams 3a, b and d are quadratically divergent, while diagram 3c is only logarithmically divergent. At this point we must warn that, quite in general, the present calculation shows lack of an appropriate chiral expansion as an expansion in the number of loops; this is due to the presence of a heavy meson ( $K^*$ ) in the loop. Hence, in contrast to calculations involving light mesons or stable heavy baryons carried out using chiral perturbation theory, in the present case multi-loop contributions contain pieces which are leading in the low energy expansion.

We regulate the loops by using a convenient form factor. One could instead have used dimensional regularization as is usually done in Chiral Perturbation Theory. This procedure, however, will require the introduction of counterterms which are unknown in the present case. Instead, the use of form factors is more likely to give a good estimate of loop contributions even when counterterms are disregarded. In the present case, we are concerned with a matrix element of the strangeness vector current operator, and, as mentioned before, only matrix elements of the octet piece of the strangeness current are affected by the one loop corrections. Consequently, one could have related the octet piece of the strangeness vector current matrix elements to similar matrix elements involving the electromagnetic current. This is, however, not good enough due to important SU(3) breaking effects in the loops produced by the mass splittings in the octets of pseudoscalar and vector mesons. For this reason we choose in this work to perform the calculation of the loop corrections to both strangeness and electromagnetic current matrix elements using the aforementioned form factors. As it is made clear later, vector current Ward identities will be properly restored while implementing the form factor.

For purposes of simplicity, we choose the form factor to depend only on  $k^2$ , the momentum squared of the virtual K-meson, and use the same cut-off mass parameter for all types of vertices. We expect this choice to be of little significance concerning the generality of our results. The hadronic form factor is taken to be

$$F(k^2) = \frac{M_K^2 - \Lambda^2}{k^2 - \Lambda^2 + i\epsilon}, \quad (23)$$

where the scale  $\Lambda$  will be chosen within a reasonable range as discussed below. For  $k^2 = M_K^2$ , one has  $F(M_K^2) = 1$ . Hence, this choice for the form factor is consistent with the values of the mesonic coupling constants ( $R_0, R_8, \xi_8$ ) extracted from on-shell amplitudes.

The implementation of this form factor in the diagrams where the current is inserted in the meson line (3c,d) is performed by the following straightforward procedure: if  $G(M_K^2, M_{K^*}^2)$  denotes the diagram for point-like hadronic vertices ( $F(k^2) \equiv 1$ ), then the corresponding diagram with  $F(k^2)$  as given in Eq. (23) is

$$\hat{\mathcal{F}}(\Lambda) [G(M_K^2, M_{K^*}^2) - G(\Lambda^2, M_{K^*}^2)], \quad (24)$$

where the operator  $\hat{\mathcal{F}}$  is given by

$$\hat{\mathcal{F}}(\Lambda) = -(\Lambda^2 - M_K^2)^2 \frac{\partial}{\partial \Lambda^2} \frac{1}{M_K^2 - \Lambda^2}. \quad (25)$$

We note that, on general grounds, the introduction of an additional momentum-dependence at the vertices also requires the inclusion of new "seagull" vertices in order to maintain gauge invariance [31, 32, 24]. In the present case, these seagull terms generate additional terms in the  $VPP\nu$  and  $VVP\nu$  interactions given in Eqs. (20) and (22). Although there exists no unique prescription for maintaining gauge-invariance in the presence of hadronic form factors, we follow the minimal prescription of Refs. [31, 32, 24] to derive our seagull terms. To this end, one may consider the form factors appearing at the hadronic vertices as arising from a co-ordinate space interaction of the form

$$\Psi(\phi_1, \dots, \phi_k)_\lambda F(-\partial^2) \partial^\lambda \Pi, \quad (26)$$

where  $\Pi$  is the octet of pseudoscalar meson fields defined in Eq. (7),  $\Psi_\lambda$  is a Lorentz vector constructed from the other pseudoscalar and vector meson fields,

and  $\partial^2$  is the D'Alembertian. Transforming to momentum space yields the same hadronic vertices as generated by the effective Lagrangians in Eqs. (13-14) multiplied by the form factor  $F(k^2)$ , where  $k$  is the momentum of the pseudoscalar meson associated with the field  $\Pi$ . The gauge invariance of this interaction can be restored by making the minimal substitution  $\partial_\mu \rightarrow D_\mu = \partial_\mu - i\hat{q}v_\mu$ , where  $\hat{q}$  is either the EM or strangeness charge operator and  $v_\mu$  is the corresponding source field. Expanding the resultant interaction to first order in  $v_\mu$  yields the seagull interaction

$$\Psi(\phi_1, \dots, \phi_k)_\lambda \left\{ v \cdot (Q + 2i\partial) \left[ \frac{F(-\Delta^2) - F(-\partial^2)}{(-\Delta^2) - (-\partial^2)} \right] \partial^\lambda [\hat{q}, \Pi] - iv^\lambda F(-\Delta^2) [\hat{q}, \Pi] \right\} \quad (27)$$

Here,  $\Delta^2 = \partial^2 - 2iQ \cdot \partial - Q^2$ , where  $Q$  is the momentum carried by the source. Transforming to momentum space, replacing the source by the associated vector boson polarization vector  $\epsilon_\mu(Q)$ , and taking the specific form for the form factor given in Eq. (23) leads to the vertex structure

$$-i\tilde{\Psi}_\lambda \left\{ \mp F(k^2) \left[ \frac{(Q \pm 2k)^\mu}{(Q \pm k)^2 - \Lambda^2} \right] k^\lambda \epsilon_\mu(Q) + F((Q \pm k)^2) \epsilon^\lambda(Q) \right\} [\hat{q}, \lambda^a] \quad , \quad (28)$$

where the SU(3) index "a" is associated with the pseudoscalar meson carrying the momentum  $k$ ,  $\tilde{\Psi}_\lambda$  is the momentum-space form for the  $\Psi_\lambda$  (without the field operators), and the upper (lower) sign corresponds to an incoming (outgoing) pseudoscalar meson.

Inclusion of this "minimal" seagull vertex (via diagrams 3a,b) is sufficient to preserve the gauge invariance of the loop calculation in the presence of hadronic form factors (for a demonstration of this feature for the case of meson-baryon loops, see Refs. [24, 26, 23]). One may, of course, include additional transverse seagull terms, which are separately conserved and which, therefore, do not modify the gauge-invariance of the calculation. At leading order in the low energy expansion we have already included the only possible seagull term, namely the term proportional to  $\zeta_8$  in  $\mathcal{L}_{VPPV}$ . Thus, other transverse seagull terms will be of higher order, and for this reason they can be disregarded.

In general, the inclusion of hadronic form factors also destroys the chiral invariance of the calculation, since the interaction in Eq. (26) is not invariant under a local chiral rotation. Restoration of chiral invariance would necessitate replacement of the derivatives  $\partial_\mu$  acting on  $\Pi$  by the chiral covariant derivative  $\nabla_\mu$

introduced in Eq. (10). Since the vector connection  $\Gamma_\mu$  appearing in  $\nabla_\mu$  can be expanded in a power series in the pseudoscalar meson field  $\Pi$ , this prescription for maintaining chiral symmetry would generate new chiral seagull vertices containing additional pseudoscalar mesons. The chiral seagull vertex of lowest order in  $1/F_0$  would contain two additional pseudoscalar meson fields and, consequently, would first contribute to the transition form factor at two-loop order. Since we restrict our attention to one-loop results, we do not consider contributions from these chiral seagull interactions.

In the notation introduced in the previous section, the VMD piece of this form factor is given by

$$\frac{1}{M_\rho} g_{\rho\pi}^{(s)}(Q^2 = 0) \Big|_{\phi\text{-dom}} = -\frac{3}{F_0} \left( \frac{4}{\sqrt{3}} R_8 \sin \theta - R_0 \cos \theta \right) \frac{1}{f_\phi} \quad (29)$$

It is convenient to use the measured rate for  $\phi \rightarrow \rho\pi$ , which gives:

$$\frac{1}{M_\rho} g_{\rho\pi}^{(s)}(Q^2 = 0) \Big|_{\phi\text{-dom}} = -\frac{3}{f_\phi} G_{\rho\phi\pi}^{\text{Phen}} \quad (30)$$

with  $G_{\rho\phi\pi}^{\text{Phen}} = 1.08 \text{ GeV}^{-1}$ . As shown in the Appendix, we can use Eq. (30) to determine the combination of  $R_0$  and  $R_8$  which appears in Eq. (29).

The one-loop contributions turn out to affect only the octet piece of the strangeness current. This is easily inferred from the effective Lagrangians containing the strangeness source  $S_\mu$ : the source always appears in a commutator, which obviously eliminates its coupling to the SU(3) singlet component of the strangeness current. We denote the one-loop contributions by  $g_{\rho\pi}^{(j)}(Q^2, k_1^2, k_1 \cdot Q) \Big|_{1\text{-loop}}^{(j)}$ , where  $j = a, b, c, d$  refers to the different diagrams, and where the dependence on  $k_1^2$  and  $k_1 \cdot Q$  allow for off-shell initial and final state mesons. In order to give the expressions of these contributions in a convenient form, we introduce an operator to project out the coefficients multiplying terms proportional to  $k_1^\alpha$  or  $Q^\alpha$  resulting from the loop integrals:

$$\hat{P}_\alpha(p, q) = \frac{p^2 q_\alpha - p \cdot q p_\alpha}{p^2 q^2 - (p \cdot q)^2} \quad (31)$$

We then have that  $\hat{P}_\alpha(p, q)p^\alpha = 0$ ,  $\hat{P}_\alpha(p, q)q^\alpha = 1$ .

The expressions for the different diagrams then read as follows:

$$\begin{aligned}
\frac{1}{M_\rho} g_{\rho\pi}^{(a)}(Q^2, k_1^2, k_1 \cdot Q) \Big|_{1-loop}^{(a)} &= \frac{4 R_8}{F_0^3} \int \frac{d^4 k}{(2\pi)^4} \frac{1}{(k^2 - M_K^2)((k_1 - k)^2 - M_K^2)} \\
&\times \left\{ \frac{1}{2} (\xi_8 - \zeta_8) F(k)^2 k^2 - \xi_8 F(k) F(k+Q) \right. \\
&\times \left[ \frac{k^2}{4} \left( -1 + 2 \frac{k \cdot (k_1 - k)}{k^2 - \Lambda^2} \right) \right. \\
&\left. \left. + \hat{P}_\alpha(k_1, Q) k^\alpha (k_1 + Q) \cdot (k_1 - k) \right] \right\} \\
\frac{1}{M_\rho} g_{\rho\pi}^{(b)}(k_1^2, k_1 \cdot Q) \Big|_{1-loop}^{(b)} &= \frac{2 R_8}{F_0^3} \xi_8 \int \frac{d^4 k}{(2\pi)^4} \frac{F(k) F(k-Q)}{(k^2 - M_K^2)((k_1 + Q - k)^2 - M_K^2)} \\
&\times \left\{ k \cdot (k_1 + Q - k) \left( 1 - \frac{1}{2} \frac{k^2}{k^2 - \Lambda^2} \right) \right. \\
&- \hat{P}_\alpha(k_1, Q) k^\alpha \left( (k_1 + Q)^2 + k \cdot (k - 2(k_1 + Q)) \right) \\
&\left. - \hat{P}_\alpha(Q, k_1) k^\alpha \left( 2(k_1 + Q)^2 + k \cdot (k - 3(k_1 + Q)) \right) \right\} \\
\frac{1}{M_\rho} g_{\rho\pi}^{(c)}(Q^2, k_1^2, k_1 \cdot Q) \Big|_{1-loop}^{(c)} &= -\frac{4 R_8 \xi_8}{F_0^3} \int \frac{d^4 k}{(2\pi)^4} F^2(k) \\
&\times \frac{1}{(k^2 - M_K^2)((k_1 - k)^2 - M_K^2)((k_1 + Q - k)^2 - M_K^2)} \\
&\times \left\{ (1 + 4z) \hat{P}_\alpha(Q, k_1) k^\alpha \right. \\
&\times [Q \cdot k (p_1 + Q) - Q \cdot (k_1 + Q) k] \cdot (k_1 - k) \\
&\left. + \frac{k^2}{4} [-(1 + 4z) (k_1 + Q)^2 + (3 + 4z) k \cdot (k_1 + Q)] \right\} \\
\frac{1}{M_\rho} g_{\rho\pi}^{(d)}(Q^2, k_1^2, k_1 \cdot Q) \Big|_{1-loop}^{(d)} &= \frac{4 R_8 \xi_8}{F_0^3} \\
&\times \int \frac{d^4 k}{(2\pi)^4} \frac{F^2(k) k^2 (k_1 - k)^2}{(k^2 - M_K^2)((k+Q)^2 - M_K^2)((k_1 - k)^2 - M_K^2)}
\end{aligned}$$

where the vector meson propagator used is as usual:

$$-i(g_{\mu\nu} - \frac{k_\mu k_\nu}{M_V^2}) / (k^2 - M_V^2 + ic).$$

For purposes of comparison we also consider the one-loop contributions to the matrix elements of the electromagnetic current  $\langle \rho(k_1, \epsilon) | J_\mu^{EM} | \pi(k_2) \rangle$  and

$\langle K^*(k_1, \epsilon) | J_\mu^{EM} | K(k_2) \rangle$ . The one-loop contributions in the case of the electromagnetic current are related to those already obtained above in a simple manner. With obvious notation, ( $f$  and  $d$  are structure constants of SU(3)), one has:

$$\begin{aligned}
g_{VP}^{(\gamma)} \Big|_{1-loop} &= -\frac{eM_V}{M_\rho} \\
&\times \sum_{a,b,c=1}^8 dV_{ab} f_{Pac} (f_{3bc} + \frac{1}{\sqrt{3}} f_{8bc}) g_{\rho\pi}^{(s)} \Big|_{1-loop} (M_{K^*} \rightarrow M_{V^*}, M_K \rightarrow M_{P^*})
\end{aligned} \tag{33}$$

It is interesting to notice that the one-loop contributions to  $g_{\rho\pi}^{(\gamma)}$  are due purely to strange particles in the loop. Only the isosinglet piece of the electromagnetic current contributes here, allowing us to write:  $g_{\rho\pi}^{(\gamma)} \Big|_{1-loop} = -\frac{e}{2} g_{\rho\pi}^{(s)} \Big|_{1-loop}$ . This one-loop correction clearly cannot be the source of explanation for the difference between  $g_{\rho^0\pi^0}^{(\gamma)}$  and  $g_{\rho^+\pi^+}^{(\gamma)}$  experimentally observed. On the other hand, the contributions to  $g_{K^*K}^{(\gamma)} \Big|_{1-loop}$  are more complicated, with contributions from both pions and Kaons in the loop. Moreover, both, isosinglet and isovector pieces of the electromagnetic current contribute, leading to different one loop corrections for charged and neutral cases.

## V. RESULTS

In this section we present and discuss the results for the one-loop contributions to the transition matrix elements of both electromagnetic and strangeness currents. Throughout we use  $R_8 = 0.27$ ,  $\xi_8 = 0.18$ ,  $z = 0$ , and,  $\zeta_8 = 0.16$  (case 1) and  $\zeta_8 = -0.08$  (case 2). Since diagram (c) turns out to give only a modest contribution, the choice  $z = 0$  has little impact on the results (we have explicitly checked that by setting  $z = \mathcal{O}(1)$  the overall one loop corrections considered in the following are affected by less than 15 %). On the other hand, if we instead use  $\xi_8 = 0.14$ , as obtained by considering  $K^*$  decay, the results obtained for  $\zeta_8$  and the final results of the loop calculation are only slightly affected.

We discuss first the case of the electromagnetic current matrix elements. To this end, it is convenient to define the ratio of the one-loop contribution to the form factor to the measured form factor ("Phen")

$$R_{VP}^{(\gamma)} \equiv \frac{g_{VP}^{(\gamma)}(\text{loop})}{g_{VP}^{(\gamma)}(\text{Phen})} \quad (34)$$

The overall sign of this ratio is undetermined, since the sign of the low energy coupling constants involved cannot be established from available observables. Hence, we consider a particular choice of the overall sign, keeping in mind that in reality the sign might be the opposite. The ratio  $R_{VP}^{(\gamma)}$  is shown in Figs. 4 and 5 for the cases of  $\rho$ -to- $\pi$  and  $K^*$ -to- $K$  radiative transitions respectively. At this point it is convenient to stress that for almost the whole allowed range of the cutoff,  $g_{\rho\pi}^{(\rho)}(\text{loop})$ ,  $g_{\rho\pi}^{(\gamma)}(\text{loop})$ ,  $g_{K^*K}^{(\gamma)}(\text{loop})$  and  $g_{K^*K}^{(\rho)}(\text{loop})$  have relative signs as follows: -1, +1, +1, +1. For  $\Lambda < 0.5$  GeV the two latter signs change in case 2 only. As shown in the appendix, the corresponding VMD pieces have the relative signs: -1, +1, +1, -1.

In each case, the choice of a "reasonable range" for the mass parameter  $\Lambda$  was dictated by two criteria. First, in order to maintain consistency with our use of VMD in extracting some of the coupling constants from radiative transitions, we require  $\Lambda$  to fall within a range such that  $R_{\rho\pi}^{(\rho)} \leq 1/2$  and  $R_{K^*K}^{(\rho)} \leq 1/2$  ( $R_{VP}^{(\gamma)} = 1/2$  corresponds to loop and vector meson poles giving equal contributions if the signs of the contributions are the same). This condition gives an upper bound of roughly one GeV. Second, to obtain a lower bound on  $\Lambda$ , we refer to a "cloudy bag" picture of hadrons in which the pseudoscalar Goldstone bosons live outside a hadronic bag containing quarks. In this picture, the virtual meson must have a wavelength longer than the bag radius, so as to be unable to penetrate the bag interior. From this requirement, we obtain a lower bound of  $\Lambda \sim 1/R_{\text{bag}} \approx 0.2$  GeV for a bag radius of one Fermi. For this choice of  $\Lambda$ , the form factor in Eq. (23) will suppress contributions from virtual pseudoscalar mesons with wavelengths shorter than one Fermi. We emphasize that although we do not perform this calculation within the cloudy bag framework, we simply turn to that picture to obtain a physical argument for a reasonable lower bound on the cutoff mass.

For  $\Lambda$  falling within our "reasonable range", the diagrams contributing to the  $\rho\pi\gamma$  form factor display a zero at  $\Lambda = M_K$ . This zero results from the numerator in Eq. (23), which was chosen to give the normalization  $F(M_K^2) = 1$ . Hence, this zero should be taken as an un-physical artifact of the choice of form factor. We believe that the values of  $R_{VP}^{(\gamma)}$  at  $\Lambda \sim 0.2$  GeV give a realistic lower bound, since this value on  $\Lambda$  is sufficiently far from the artificial zero at  $M_K$ . In order to check this assumption, we also computed the diagrams with a slightly different form

factor, replacing the numerator of Eq. (23) with  $-\Lambda^2$ . Such a form factor also displays pointlike behavior ( $F(k^2) = 1$ ) as  $\Lambda \rightarrow \infty$ . The resulting values of  $R_{VP}^{(\gamma)}$  for  $\Lambda$  in the vicinity of  $M_K$  do not differ significantly from those obtained with the form in Eq. (23) and  $\Lambda \sim 0.2$  GeV. In the case of the  $K^* \rightarrow K\gamma$  form factor, no zero appears at  $\Lambda = M_K$  since loops involving virtual pions also contribute. The latter enter with hadronic form factors normalized to unity at  $k^2 = m_\pi^2$  and, thus, do not vanish at  $\Lambda = M_K$ .

The one-loop contribution in the  $\rho\pi\gamma$  case is about 2-5 % when  $\Lambda \sim 0.7$  GeV, and grows to 20-35% for  $\Lambda \sim 1$  GeV (see Fig. 4). Thus, we take roughly 1 GeV as an upper bound for our reasonable range for  $\Lambda$ . For the  $K^*K\gamma$  form factor, the loops containing a  $\pi$  and a  $K^*$  in the intermediate state are the dominant ones. The loop contributions are relatively more important than in the case of the  $\rho\pi\gamma$  form factor. For charged Kaons we find the one loop contribution to be 0-15 % for  $\Lambda \sim 0.7$  GeV and 20-60 % for  $\Lambda \sim 1$  GeV, while for neutral Kaons the corresponding contributions are 0-10 % and 20-50 % (see Fig. 5). Notice that our analysis relies on VMD to determine some low energy constants, like  $R_8$  and  $R_0$  (see the Appendix). Large one loop contribution to the radiative decays would demand performing a self-consistent fitting procedure, in which both VMD and one-loop amplitudes are included in the determination of  $R_8$  and  $R_0$ . Such an analysis would become imperative if the cutoff would be taken larger than about 1 GeV. Notice that if a new fit would be required, this should be done twofold due to our ignorance about the overall sign of the one loop corrections. Although a shift in the value used for  $R_8$  will result from the loop corrections, we expect that for our choice of cutoff scale such a shift will not qualitatively alter our main conclusions.

For the strangeness vector current transition form factor, we must define a somewhat different ratio since  $g_{\rho\pi}^{(\rho)}(Q^2)$  has not been measured. We compute instead ratio  $\tilde{R}_{\rho\pi}^{(\rho)}$  of one-loop to vector meson dominance contributions

$$\tilde{R}_{\rho\pi}^{(\rho)} \equiv \frac{g_{\rho\pi}^{(\rho)}(\text{loop})}{g_{\rho\pi}^{(\rho)}(\text{VMD})} \quad (35)$$

The results for the ratio  $\tilde{R}_{\rho\pi}^{(\rho)}$ , shown in Fig. 6, turn out to be significant almost for any value cutoff mass within the chosen range. The reason is that  $\left|g_{\rho\pi}^{(\rho)}(Q^2 = 0)\right|_{\phi\text{-dom}}$  is very small ( a factor three smaller than  $1/e g_{\rho\pi}^{(\gamma)\text{Phen}}$  ), while the absolute value of the one-loop correction is a factor two larger than

$1/e g_{\rho\pi}^{(\gamma)} \Big|_{1-loop}$ ; thus, the corresponding ratio is almost a factor six larger than in  $\rho\pi\gamma$  case. Consequently, for  $\Lambda \sim 1$  GeV, the strangeness  $\rho - \pi$  transition matrix element can be as large in magnitude as the corresponding EM transition matrix element, assuming the loop and  $\phi$ -pole contributions enter with the same sign (uncertain at present). For small values of the form factor mass ( $\Lambda \sim 0.2$  GeV), however, the loop correction to the  $\phi$ -pole contribution is 50% at most, in which case  $g_{\rho\pi}^{(\rho)}(0)$  is no more than half as large as  $g_{\rho\pi}^{(\gamma)}(0)$ .

In addition to giving the  $\Lambda$ -dependence of  $\tilde{R}_{\rho\pi}^{(\rho)}$ , the curves in Fig. 6 also illustrate the sensitivity of our results to other parameters which enter. As in the case of  $g_{\rho\pi}^{(\gamma)}(0)$ , the dependence of the strangeness form factor on the choice of low-energy constant  $\zeta_8$  is modest: the lower set of curves (case 1) and upper set (case 2) differ by less than a factor of two over our reasonable range for  $\Lambda$ . Similarly, the dependence on the  $\rho$  and  $\pi$  virtuality is negligible, as a comparison of the solid curves ( $k_1^2 = m_\rho^2$ ,  $k_2^2 = m_\pi^2$ ) and dashed curves ( $k_1^2 = 0$ ,  $k_2^2 = 0$ ) indicates. For this reason, we conclude that a nuclear MEC calculation carried out using  $k_1^2 = m_\rho^2$  and  $k_2^2 = m_\pi^2$  in  $g_{\rho\pi}^{(\rho)}$  rather than allowing these momenta to vary introduces negligible error.

Finally, we refer to the dash-dotted curve, which gives the ratio  $\tilde{R}_{\rho\pi}^{(\rho)}$  (for case 1) at the kinematics of the approved CEBAF experiment [14],  $-Q^2 = 0.6$  GeV<sup>2</sup>. In this case the  $\phi$ -pole contribution to  $g_{\rho\pi}^{(\rho)}(Q^2)$  is down from its value at the photon point by  $(1 - Q^2/m_\phi^2)^{-1} \approx 0.6$ . The ratio  $\tilde{R}_{\rho\pi}^{(\rho)}$ , on the other hand, is essentially unchanged from its value at the photon point. Thus, we would expect the loop contributions to modify the strangeness MEC results of Refs. [27, 28] by a factor of between 0.1 and 3.5 (for  $\Lambda$  varying over our reasonable range) over the complete range of  $Q^2$  considered in those calculations.

These results have significant implications for the interpretation of CEBAF experiment [14]. Assuming, for example, that the nucleon's strangeness form factors were identically zero, PV <sup>4</sup>He asymmetry would still differ from its "zero-strangeness" value [ $F_0^{(\rho)}(0) = 0$  in Eq. (1)] by roughly 15-40% due to the  $\rho - \pi$  strangeness MEC. Thus, for purposes of extracting limits on the nucleon's strangeness electric form factor, one encounters about a 25% theoretical uncertainty associated with non-nucleonic strangeness. By way of comparison, we note that models which give a large nucleon strangeness electric form factor,  $|G_E^{(\rho)}/G_E^n| \sim 1$  generate a 20% correction to  $A_{LN}$  via the one- and two-body mechanisms of Fig. 1a,b. On the other hand, given the projected 40% experimental error for the CEBAF measurement, a statistically significant non-zero result

for  $F_0^{(\rho)}$  would signal the presence of both a large strange-quark content of the nucleon as well as a large, non-nucleonic strange-quark component of the nucleus.

## VI. SUMMARY AND CONCLUSIONS

We have calculated vector-to-pseudoscalar meson vector current form factors using a combination of vector meson pole and one one-loop contributions. As expected, the one-loop results are strongly dependent on the mass parameter in the hadronic form factor needed to regulate otherwise divergent loop integrals. For values of  $\Lambda$  lying within a "reasonable range" whose upper limit is determined by self-consistency with VMD and lower limit by a cloudy bag picture of hadrons, we find that the one-loop contributions to the  $\rho\pi\gamma$  and  $K^*K\gamma$  amplitudes may introduce important corrections to the predictions of VMD model. In the case of the strangeness vector current  $\rho$ -to- $\pi$  transition form factor, the loop contributions may enhance the total amplitude by more than a factor of three over the estimate based on VMD. Assuming loops involving heavier mesonic intermediate states do not cancel the contribution from the lightest mesons, our results could have serious implications for the interpretation of the moderate- $|Q^2|$ , CEBAF PV electron scattering experiment with a <sup>4</sup>He target [14]. Indeed, this strangeness transition form factor, which contributes to the nuclear strangeness charge form factor  $F_0^{(\rho)}(q)$  via a meson exchange current [27, 28], would induce a 15 - 40% correction to the zero-strangeness <sup>4</sup>He PV asymmetry [Eq. (1) with  $F_0^{(\rho)} = 0$ ]. Were the measurement [14] to extract a statistically significant, non-zero result for  $F_0^{(\rho)}$ , one would have evidence that non-valence quark degrees of freedom — both nucleonic and non-nucleonic — play an important role in the medium energy nuclear response.

## VII. ACKNOWLEDGEMENTS

J.L.G. was supported by NSF grant HRD-9154080 and by DOE contract DE-AC05-84ER40150. M.J.M. was supported by NSF NYI award PIY-9357484 and DOE contracts DE-AC05-84ER40150 and DE-FG05-94ER0832.

## VIII. APPENDIX

In this appendix we describe the determination of  $R_0$  and  $R_8$ .

Determination of  $R_0$  and  $R_8$ : these two effective couplings can be determined by using the decay width of  $\phi \rightarrow \rho\pi$  and the radiative decays of vector mesons supplemented with the hypothesis of VMD.

The partial width  $\Gamma(\phi \rightarrow \rho\pi)$  is given by:

$$\Gamma(\phi \rightarrow \rho\pi) = \frac{|G_{\phi\rho\pi}|^2}{12\pi} |k_f|^3.$$

From eq. (13) we obtain:

$$G_{\phi\rho\pi} = \frac{1}{F_0} \left( -R_0 \cos\theta + \frac{4}{\sqrt{3}} R_8 \sin\theta \right),$$

while the experimentally observed partial width gives:

$$|G_{\phi\rho\pi}^{\text{phen}}| = 1.08 \text{ GeV}^{-1}.$$

In practice we will take  $\theta$  to correspond to ideal  $\phi - \omega$  mixing.

The radiative transition amplitude  $V \rightarrow P\gamma$  has the general form:

$$A(V \rightarrow P\gamma) = -i g_{VP}^{(\gamma)} \epsilon_{\mu\nu\rho\sigma} P_V^\mu \epsilon_V^\nu P_P^\rho \epsilon_\gamma^\sigma.$$

The radiative partial width is given by:

$$\Gamma(V \rightarrow P\gamma) = \frac{\alpha}{3} \left| \frac{g_{VP}^{(\gamma)}}{M_V} \right|^2 |k_f|^3.$$

Using VMD we have that:

$$g_{VP}^{(\gamma)}(Q^2) = -M_V \sum_{V'=\rho^0, \omega, \phi} \frac{G_{VV'P} C_{V'}}{Q^2 - M_{V'}^2},$$

where  $C_V = M_V^2/f_V$ ,  $f_\rho = 5.1$ ,  $f_\omega = 17$ , and  $f_\phi = 13$ . From eq. (13) we obtain:

$$G_{\rho\rho\pi} = 0$$

$$G_{\rho\omega\pi} = \frac{1}{F_0} \left( \frac{4}{\sqrt{3}} R_8 \cos\theta + R_0 \sin\theta \right)$$

$$G_{\rho\phi\pi} = \frac{1}{F_0} \left( \frac{4}{\sqrt{3}} R_8 \sin\theta - R_0 \cos\theta \right)$$

$$G_{K^*+\rho K^+} = \frac{2}{F_0} R_8$$

$$G_{K^*+\omega K^+} = \frac{1}{F_0} \left( -\frac{2}{\sqrt{3}} R_8 \cos\theta + R_0 \sin\theta \right)$$

$$G_{K^*+\phi K^+} = -\frac{1}{F_0} \left( \frac{2}{\sqrt{3}} R_8 \sin\theta + R_0 \cos\theta \right)$$

$$G_{K^*0\rho K^0} = -G_{K^*+\rho K^+}$$

$$G_{K^*0\omega K^0} = G_{K^*+\omega K^+}$$

$$G_{K^*0\phi K^0} = G_{K^*+\phi K^+}$$

The effective couplings  $g_{VP}^{(\gamma)}(Q^2 = 0)$  determined from the various radiative decays and defined by turn out to be:

$$g_{\rho^0\rho^0}^{(\gamma)} = 0.753, \quad g_{\rho^+\rho^+}^{(\gamma)} = 0.568, \quad g_{K^*0K^0}^{(\gamma)} = -1.13,$$

$$g_{K^*+K^+}^{(\gamma)} = 0.75, \quad g_{\omega\pi^0}^{(\gamma)} = 1.81, \quad g_{\phi\pi^0}^{(\gamma)} = -0.14$$

where the relative signs are chosen to match those predicted by VMD. Using these phenomenological results, our best VMD fit leads to:

$$R_0 \sim 1.0, \quad R_8 \sim 0.27.$$

These fitted values give the VMD results for  $g_V^{(\gamma)}$ :

$$0.55, \quad 0.55, \quad -1.27, \quad 0.76, \quad 1.91, \quad -0.15$$

to be compared with the respective phenomenological values given above.

The VMD result for the transition matrix elements of the strangeness current have the same structure, the only difference is that now  $C_V$  has to be replaced by  $S_V$ . In the following we assume that  $S_V$  is only non-vanishing for  $V = \phi$ . This holds whenever  $C_0$  corresponds to exact OZI suppression as mentioned in section III. From eq. (16) we obtain:

$$S_\phi = -3 \frac{M_\phi^2}{f_\phi}.$$

This leads to the VMD result used in the text:

$$\frac{1}{M_\rho} g_{\rho\pi}^{(*)}(Q^2 = 0) \Big|_{\phi\text{-dom}} = \frac{1}{M_\phi^2} G_{\rho\phi\pi}^{\text{Phen}} S_\phi.$$

From the results quoted above, VMD predicts the following pattern of signs:

$$g_{\rho\pi}^{(\gamma)} > 0, \quad g_{K^*0 K^0}^{(\gamma)} < 0, \quad g_{K^*+ K^+}^{(\gamma)} > 0,$$

$$g_{\omega\pi^0}^{(\gamma)} > 0, \quad g_{\phi\pi^0}^{(\gamma)} < 0, \quad g_{\rho\pi}^{(*)} < 0.$$

- [3] W. M. Alberico et al., *Nucl. Phys.* A560 (1994) 701.
- [4] T. W. Donnelly et al., *Nucl. Phys.* A541 (1992) 525.
- [5] D. H. Beck, *Phys. Rev.* D39 (1989) 3248.
- [6] M. J. Musolf and T. W. Donnelly, *Z. Phys.* C57 (1993) 559.
- [7] E. J. Beise and R. D. McKeown, *Comments Nucl. Part. Phys.* 20 (1991) 105.
- [8] D. B. Kaplan and A. Manohar, *Nucl. Phys.* B310 (1988) 527.  
J. Napolitano, *Phys. Rev.* C43 (1991) 1473.
- [9] G. T. Garvey et al., *Phys. Lett.* B280 (1992) 249.
- [10] G. T. Garvey, W. C. Louis, and D. H. White, *Phys. Rev.* C48 (1993) 761.
- [11] G. T. Garvey et al., *Phys. Rev.* C48 (1993) 1919.
- [12] C. J. Horowitz et al., *Phys. Rev.* C48 (1993) 3078.
- [13] MIT-Bates Proposal # 89-06, R. D. McKeown and D. H. Beck, contact persons (unpublished).
- [14] CEBAF Proposal # PR-91-004, E. J. Beise, spokesperson (unpublished).
- [15] CEBAF Proposal # PR-91-010, J. M. Finn and P. A. Souder, spokespersons (unpublished).
- [16] CEBAF Proposal # PR-91-017, D. H. Beck, spokesperson (unpublished).
- [17] MIT-Bates Proposal # 94-11, B. Mueller, M. Pitt, and E. J. Beise, spokespersons (unpublished).
- [18] LAMPF Proposal # 1173, LSND Collaboration, Los Alamos National Laboratory Report LA-UR-89-3764 (1989), W. C. Louis, spokesperson.
- [19] L. A. Ahrens et al., *Phys. Rev.* D35 (1987) 785.
- [20] R. L. Jaffe, *Phys. Lett.* B229 (1989) 275.
- [21] N. W. Park, J. Schechter, and H. Weigel, *Phys. Rev.* D43 (1991) 869.
- [22] B. R. Holstein, in Proc. of the Caltech Workshop on Parity Violation in Electron Scattering, E. J. Beise and R. D. McKeown, eds. (World Scientific, Singapore, 1990), pp. 27-43.
- [23] W. Koepf, E. M. Henley, and J. J. Pollock, *Phys. Lett.* B288 (1992) 11.; W. Koepf and E. M. Henley, *Phys. Rev.* C40 (1994) 2219.
- [24] M. J. Musolf and M. Burkardt, *Z. Phys.* C61 (1994) 433.
- [25] T. Cohen, H. Forkel, and M. Nielsen, *Phys. Lett.* B316 (1993) 1.
- [26] H. Forkel et al., *Phys. Rev.* C50 (1994) 3108.
- [27] M. J. Musolf and T. W. Donnelly, *Phys. Lett.* B318 (1993) 263.
- [28] M. J. Musolf, R. Schiavilla, and T. W. Donnelly, *Phys. Rev.* C50 (1994) 2173.
- [29] Particle Data Group, Review of Particle Properties, *Phys. Rev.* D50 (1994) 1173.
- [30] The value of  $g_{\rho\pi^0}$  quoted in Refs. [27, 28] is adimensional and it is related to the value given here, which has dimension two, by a factor  $m_\rho m_\phi$ .
- [31] F. Gross and D.O. Riska, *Phys. Rev.* C36 (1987) 1928.
- [32] K. Ohta, *Phys. Rev.* C40 (1989) 1335.

[1] M. J. Musolf et al., *Phys. Rep.* 239 (1994) 1.

[2] M. J. Musolf and T. W. Donnelly, *Nucl. Phys.* A546 (1992) 509; *Nucl. Phys.* A550 (1992) 564(E).

FIGURES

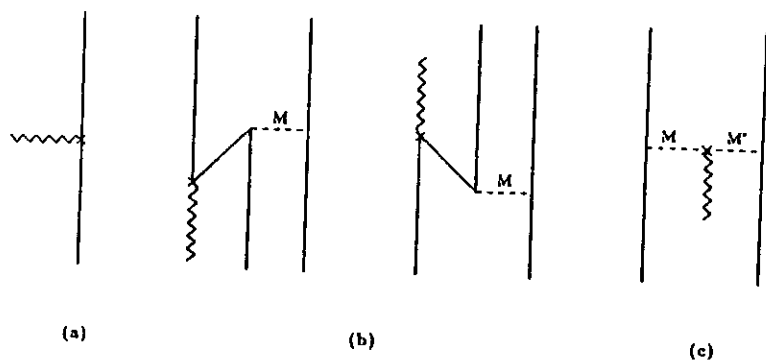


Figure 1: Contributions to the nuclear strangeness charge form factor,  $F_C^{(s)}(q)$ . One-body (a) and "pair current" (b) contributions depend on the nucleon's strange-quark vector current form factors. "Transition current" (c) contributions arise from strange-quark vector current matrix elements between meson states  $|M\rangle$  and  $|M'\rangle$ . Here, the cross indicates the insertion of the strangeness charge operator.

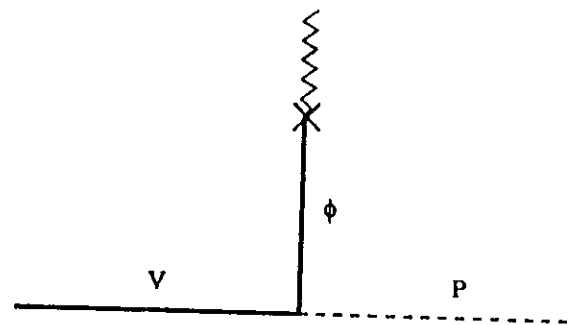


Figure 2:  $\phi$ -meson dominance picture of the strangeness current transition matrix element.  $V$  refers to a vector meson,  $P$  to a pseudoscalar, and the cross represents the insertion of the current.

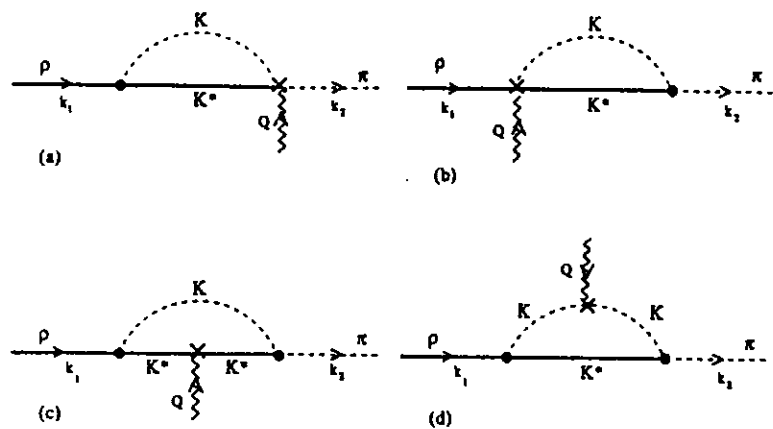


Figure 3: One-loop diagrams which contribute to the strangeness current transition matrix element. The cross represents the strangeness vector current.

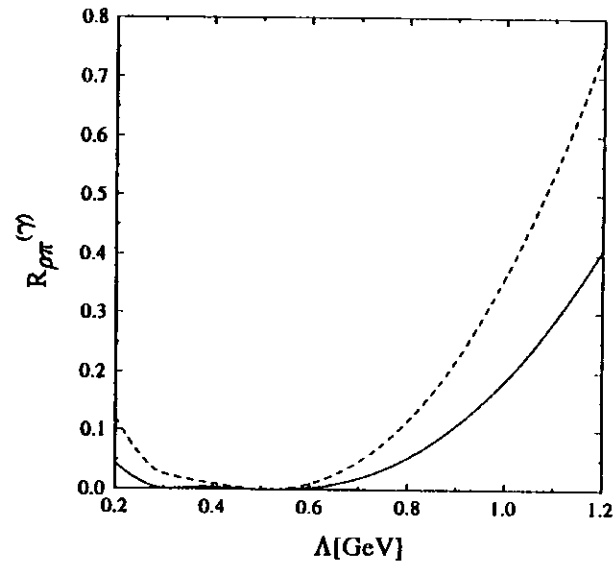


Figure 4: Ratio  $R_{\rho\pi}^{(\gamma)}$  for the matrix element of the electromagnetic current between  $\rho$  and  $\pi$  mesons. The solid curve correspond to case 1 ( $\zeta = 0.16$ ) and the dashed one to case 2 ( $\zeta = -0.08$ ). In each case we have used  $k_1^2 = M_\rho^2$ ,  $Q^2 = 0$ , and  $k_2^2 = M_\pi^2$ .

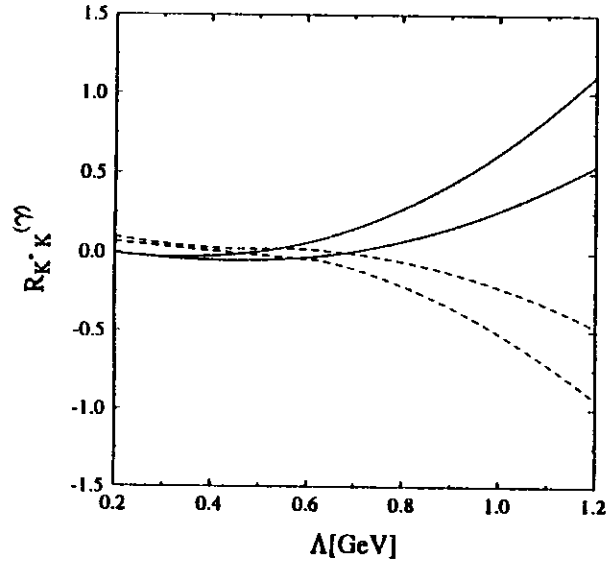


Figure 5: Ratio  $R_{K^* K}^{(\gamma)}$  for the matrix element of the electromagnetic current between  $K^*$  and  $K$  mesons. The solid lines correspond to charged kaons and the dashed ones to neutral kaons. In each case, the upper curve corresponds to case 2, and the lower one to case 1. The kinematic invariants used are:  $k_1^2 = M_{K^*}^2$ ,  $Q^2 = 0$ , and  $k_2^2 = M_K^2$ .

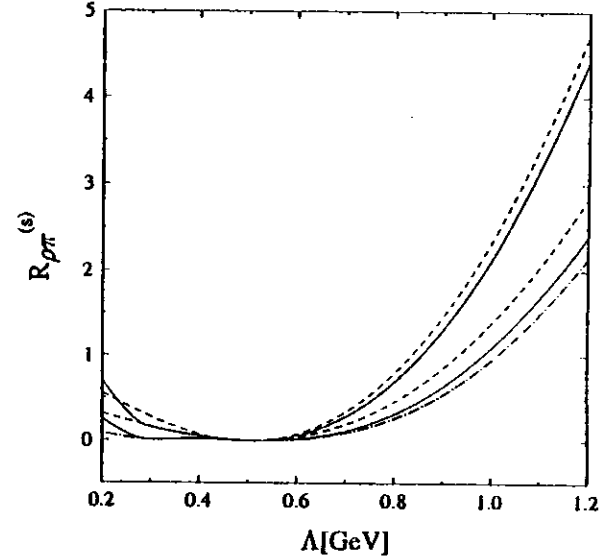


Figure 6: Ratio  $\tilde{R}_{\rho\pi}^{(s)}$  for the matrix element of the strangeness current between  $\rho$  and  $\pi$  mesons. The solid curves corresponds to case 1 and the dashed ones to case 2. In each case the lower curve corresponds to  $k_1^2 = M_\rho^2$ ,  $Q^2 = 0$  and  $k_2^2 = M_\pi^2$ , and the upper one to  $k_1^2 = 0$ ,  $Q^2 = 0$  and  $k_2^2 = 0$ . The dash-dotted curve corresponds to case 1 with  $k_1^2 = M_\rho^2$ ,  $Q^2 = 0.6 \text{ GeV}^2$  and  $k_2^2 = M_\pi^2$ , and the dotted curve corresponds to case 1 with  $k_1^2 = M_\rho^2$ ,  $Q^2 = 0$  and  $k_2^2 = M_\pi^2$ , and the form factor  $F(k^2) = \Lambda^2/(\Lambda^2 - k^2)$ .